I-V characteristics of microwave-driven Josephson junctions in the low-frequency and high-damping regime

C. Vanneste,* C. C. Chi, K. H. Brown, A. C. Callegari, M. M. Chen, J. H. Greiner, H. C. Jones, K. K. Kim, A. W. Kleinsasser, H. A. Notarys, G. Proto, R. H. Wang, and T. Yogi
IBM Thomas J. Watson Research Center, Yorktown Heights, New York 10598
(Received 27 December 1984)

Experimental I-V curves of microwave-driven Josephson tunnel junctions with resistive shunts are reported. The results are in very good agreement with numerical calculations using the resistively shunted junction model. In the low-frequency regime there are three distinct regions in the I-V curves and two different types of Shapiro steps. It is demonstrated that the overall shape of the I-V curves can be explained by using an adiabatic interpretation of the junction response. The two different types of Shapiro steps are related to a compensation effect between dc and rf bias currents.

When a Josephson junction is driven by a microwave field, two main features are experimentally observed: first a progressive changing of the overall shape of the I-V characteristic with the microwave power, and at the same time, the appearance of Shapiro steps[1] corresponding to the locking of the Josephson oscillator to the oscillating external field. Numerous experiments and theoretical calculations have been devoted to the magnitudes of the low-order Shapiro steps. A Bessel-function dependence of the steps on the microwave power is usually expected from a simple voltage source model. However, experimentally, Josephson junctions are often current-biased and deviations from the Bessel-function behavior have been reported and also predicted by using the resistively shunted Josephson-junction model (RSJ) without capacitance.[2,3] However, not much has been done in the past concerning the overall shape of the I-V characteristics of microwave-driven junctions and, to our knowledge, a physical interpretation of the non-Bessel-function behavior of the Shapiro steps and of their position on the I-V curves has not been previously reported. In this communication, we present detailed experimental results on resistively shunted Josephson junctions driven by microwave radiation in the low-frequency regime ($\omega < \omega_c$, where ω_c is the characteristic frequency given by $\omega_c = 2eRI_c/\hbar$). The shape of the I-V characteristics as well as the step behavior are not only in very good agreement with numerical simulations using the RSJ model, but are also explained in a physical way.

The 0.15×10-μm^2 Nb-Nb0_x-PbInAu edge junctions shunted by a TiAu strip used in this experiment were fabricated by Brown *et al.* using their standard processing.[4] The parasitic inductance of the resistive shunt was deliberately reduced by using a superconducting ground plane. Typical values of the junction parameters were $I_c = 0.15$ mA, $R = 2\Omega$, and $C = 0.4$ pF, where I_c, R, and C are, respectively, the critical current, the resistance, and the capacitance of the junction. Due to the low value of the Stewart-McCumber parameter $\beta_c \equiv 2eR^2CI_c/\hbar \approx 0.7$, no capacitance-induced hysteresis was observed in the I-V characteristic.[5] For $\beta_c < 1$, the junctions can be closely simulated by using the RSJ model without capacitance. The junctions were irradiated with microwaves at frequencies around 12, 18, and 36 GHz. Figure 1 shows the I-V characteristics for different microwave powers at $\nu = 18$ GHz. When the microwave power is increased, the overall shape of the I-V characteristic experiences distortion while the critical current is decreasing and Shapiro steps are induced. We note that before the zero-voltage step is reduced to zero, all the other steps are increasing progressively [Fig. 1(b)]. These steps are described as stable steps because they do not oscillate in this range of microwave power. When the zero-voltage step is first suppressed to zero by the microwaves, these steps spread over a dc current range about twice the critical current and the distortion of the I-V characteristic looks like a "bump," i.e., a concave shift from the ohmic line, in the same range [Fig. 1(c)]. When the microwave power is further increased, the bump with the nonoscillating steps shifts toward higher values of the dc current [Figs. 1(d) and 1(e)]. While the location of the bump on the I-V curve is moving, its range is always spreading over a dc current range about twice the critical current. At the same time, below this range, microwave-induced steps oscillate rapidly with increasing the microwave power and stay closely along the ohmic line. Their appearance on the I-V curves and response to the microwave power are distinct from the steps associated with the bump. To summarize, for microwave powers higher than that needed to first suppress the zero-voltage-current step to zero, three ranges can be defined in the I-V characteristic. Range I corresponds to large dc bias currents where the I-V curve asymptotically approaches the ohmic line without microwave induced steps. Range II corresponds to an intermediate dc current range in which the I-V curve deviates from the ohmic line as a concave bump with stable steps superimposed on it. Range III corresponds to the lower dc current range where the steps oscillate with microwave power along the ohmic line.

The observations just described are in good agreement with the RSJ model (Fig. 2), using the experimental parameters of the junctions in the governing equation of the phase:

$$\frac{d\phi}{d\tau}+\sin\phi=i_0+i_1\sin(\Omega\tau)\ , \tag{1}$$

where i_0 and i_1 are the dc and microwave current amplitudes normalized to the critical current, τ is the reduced time connected to the real time t by $\tau=\omega_c t$, and Ω is the microwave frequency normalized to ω_c. A careful comparison of experimental and numerical curves shows some small discrepancies. For instance, in the range I experimental curves approach the ohmic line faster than the numerical curves as the dc current increases, which is due to the small capacitance of the real junctions. A better fit of the experimental curves has been obtained by solving Eq. (1) with a small capacitative term added. However, it can be seen that the characteristic features, i.e., the bump and the two kinds of steps, are already exhibited by the simple RSJ model without capacitance. Therefore, we will limit ourselves to this case in the following discussion.

Figure 3 shows the time dependence of the voltage $d\phi/d\tau$ and of the pair current $\sin\phi$ for values of the dc current i_0 corresponding to the three ranges I, II, and III at a fixed value of the microwave current. If $i(\tau)=i_0+i_1\sin(\Omega\tau)$ is the total current in the junction at the time τ, we notice that to a good approximation the junction is following $i(\tau)$ adiabatically.[6,7] During a microwave cycle, when the total current $i(\tau)$ is in the range $(-1,+1)$, the voltage $d\phi/d\tau$ drops close to zero while the pair current carries almost all the total current [Figs. 3(b) and 3(c)]. When $i(\tau)$ is outside the range $(-1,+1)$, the voltage and the pair current oscillate at the Josephson frequency roughly corresponding to the value it should have for the junction biased with a dc current $i(\tau)$ [Figs. 3(a), 3(b), and 3(c)]. To recapitulate, during each microwave cycle, the junction is behaving itself at time τ as if it were just biased by a dc current $i(\tau)$. The smaller the reduced frequency is, the better this adiabatic behavior is approached. The characteristic frequency, which can be considered as the relaxation time of the junction, defines the high-frequency limit of this adiabatic regime. However, quasiadiabatic behavior of the junction can still be observed up to $\Omega=0.5$.

From this adiabatic picture of the junction behavior, the overall shape of the I-V characteristics (i.e., without taking account of the steps) can be computed in an easy way. Assuming that for each value of $i(\tau)$, the mean voltage $\langle d\phi/d\tau\rangle_{\rm av}$ has the value it would have for the same junction biased with a dc current $i=i(\tau)$ and knowing that for each dc bias current i_0, the total current $i(\tau)$ probes the current range i_0-i_1 to i_0+i_1 at the microwave frequency Ω, the mean voltage is given by the averaging formula:

$$\langle v\rangle_{\rm av}=(\Omega/2\pi)\int_0^{2\pi/\Omega} v_0(i)d\tau\ , \tag{2}$$

where

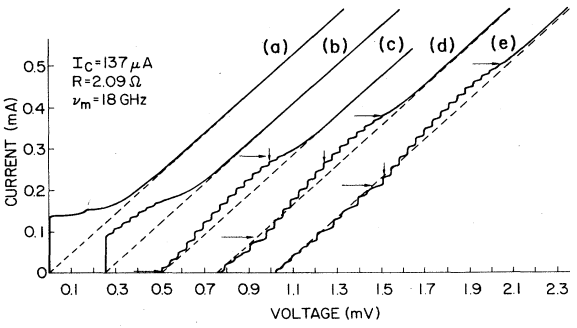

FIG. 1. Experimental I-V curves at 4.2 K for increasing microwave powers. Dashed lines represent ohmic lines. The reduced microwave frequency is $\Omega=0.13$. The large arrows indicate the dc current boundaries of the three ranges defined in the text. The small arrows show the decrease of the dc current position of a stable step ($n=13$).

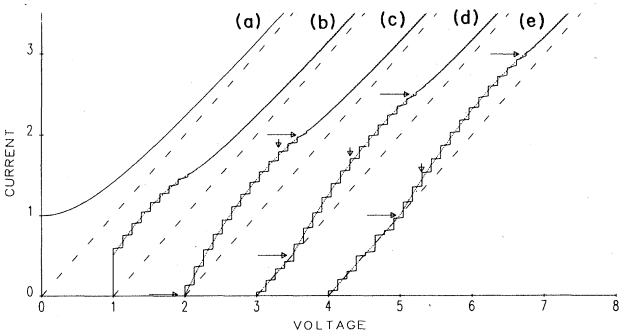

FIG. 2. Numerical I-V curves for increasing microwave currents at the reduced frequency $\Omega=0.13$. Solid lines represent solutions of the RSJ model (reduced units). Dotted lines represent solutions of Eqs. (2) and (3) (adiabatic approximation). (a) $i_1=0$, (b) $i_1=0.5$, (c) $i_1=1$, (d) $i_1=1.5$, and (e) $i_1=2$. Dashed lines represent ohmic lines. The large arrows indicate the dc current boundaries i_1-1 and i_1+1 of the three ranges defined in the text. The small arrows show the decrease of the dc current position of a stable step ($n=10$).

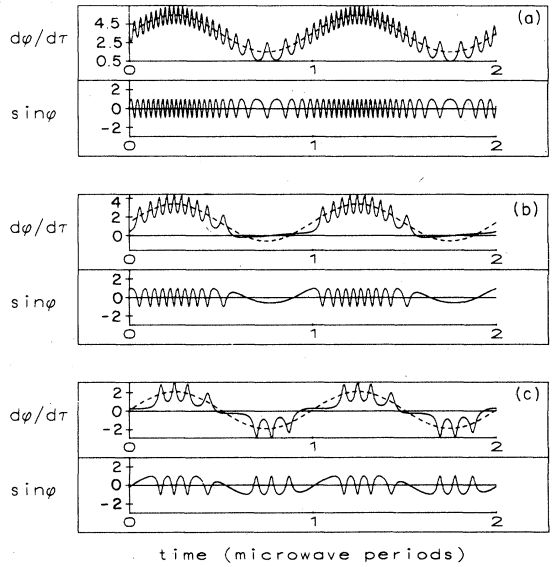

FIG. 3. Time dependence of the voltage $d\phi/d\tau$ and the pair current $\sin\phi$ (reduced units) for different values of the dc current at fixed microwave current ($i_1=2$). (a) $i_0=3.5$ (range I), (b) $i_0=1.4$ (range II), and (c) $i_0=0.1$ (range III). Dotted lines represent the total current $i(\tau)$.

$$i=i(\tau)=i_0+i_1\sin(\Omega\tau)\ ,$$

$$v_0(i)\equiv\begin{cases}\pm(i^2-1)^{1/2}, & |i|>1\\ 0, & -1\le i\le+1\ .\end{cases}\tag{3}$$

Equation (3) is the well-known solution of the I-V characteristic from Eq. (1) when $i_1=0$. Solutions of Eqs. (2) and (3) are displayed as dotted curves on Fig. 2 and show a very good agreement with the numerical solutions of the RSJ model. This agreement provides a strong support to the adiabatic picture of a Josephson junction in this low-frequency regime. The bump is then understood as due to the adiabatic averaging of the nonlinear I-V curve without microwaves [Fig. 2(a)] according to Eq. (2). For microwave currents larger than the critical current, this bump spreads approximately over the dc current range i_1-1, i_1+1 [range II, Figs. 2(c), 2(d), and 2(e)]. If i_0 is smaller than i_1-1 (range III) the total current $i(\tau)$ probes the negative part of the I-V characteristic below the negative critical current -1 [Fig. 3(c)], resulting in an average value of the pair current close to zero and a mean voltage close to the ohmic line. If i_0 is larger than i_1+1 (range I), $i(\tau)$ probes only dc current values above the positive critical current $+1$ [Fig. 3(a)]. Therefore, in this range, the I-V curve asymptotically approaches the ohmic line.

Having used the adiabatic approximation to describe the overall shape of the I-V characteristics, it is possible to go further to explain why no steps are observed in the range I, why steps are stable in the range II, and why they are oscillating in the range III. Looking at Fig. 3, each fast Josephson oscillation of $d\phi/d\tau$ and $\sin\phi$ corresponds to a 2π rotation of the phase ϕ when $i(\tau)$ is outside the range $(-1,+1)$. Inside the range $(-1,+1)$, where $d\phi/d\tau$ is close to zero, the phase is slowly evolving but does not experience 2π rotations. On a step, solutions of Eq. (1) are periodic like those exhibited on Figs. 3(b) and 3(c). In Fig. 3(b), the number of sharp Josephson oscillations per microwave cycle gives the order of the step ($n=0,1,2,\ldots$). In Fig. 3(c) as the total current probes values below -1, the phase not only experiences positive but also negative 2π rotations during a microwave cycle so that the order of the step is now given by the difference of positive and negative sharp oscillations of the voltage. At fixed microwave current i_1, a step corresponds to different solutions of Eq. (1) which remain periodic with the same number of positive and negative 2π rotations of the phase when the dc current is increased. At the top of a step, a further increase of the dc current makes a new positive 2π rotation of the phase to appear or a negative 2π rotation to disappear during the microwave cycle, which corresponds to a jump to the next step. It can be observed numerically by using Eq. (1) that in the transition regime between two steps the solutions exhibit the emergence or the disappearance of an oscillation. In the same way, fixing the dc current and increasing the microwave current will make the number of either positive or negative 2π rotations per microwave cycle to increase, corresponding to jumps to next or preceding steps.

Keeping this picture in mind, when the dc current is in range I [Fig. 3(a)], the total current stays above the critical current $+1$ during the entire microwave cycle so that the junction never probes the zero-voltage state. In this case, the number of sharp Josephson oscillations can almost change continuously with the dc current so that the dc current ranges on which the solutions of Eq. (1) stay locked on a step become vanishingly small. Experimentally due to the presence of thermal noise, it is difficult to observe steps in this range. When the dc current is in range II, the phase only experiences positive 2π rotations [Fig. 3(b)], but now the voltage stays close to zero when $i(\tau)$ is smaller than the critical value $+1$. The appearance of this zero-voltage state during the microwave cycle contributes to the locking of solutions on large steps. Looking at the nth step corresponding to n sharp Josephson oscillations in a microwave cycle, it can be seen from Fig. 3(b) that any increase of the microwave current i_1 can be counterbalanced by a decrease of the dc current i_0 in order to avoid the occurrence of a new 2π rotation of the phase. Thus, any step in this range is stable because an increase of the microwave power shifts down its dc current bias position without substantially changing its size. This process will be effective as long as the total current stays above the negative critical current -1 during a microwave cycle. The stable steps correspond to the large initial plateaus already reported in past efforts[3] when the step size is plotted versus the microwave-current amplitude. It can be shown that the microwave-current range of this plateau increases approximately from I_c for the lowest-order step to $2I_c$ for higher-order steps. The shift to lower values of the dc bias current range position of a given stable step when the microwave power is increased can be seen on both experimental and numerical curves (Figs. 1 and 2). Moreover, as these stable steps only exist in range II, they are superimposed on the bump. For dc currents in range III (this range only exists for $i_1>1$) the phase experiences both positive and negative 2π rotations [Fig. 3(c)]. If at a fixed dc current the microwave power is increased, new negative as well as new positive 2π rotations will now appear. Let us assume, for example, the junction is biased near the top of the nth-order step for a certain microwave power, and an increase of the microwave power tends to first induce a new positive 2π rotation of the phase. Trying to avoid the occurrence of this new positive 2π rotation by decreasing the dc current will make, in fact, a new negative 2π rotation to appear, which means a jump to the preceding step. Hence, in this case, the counterbalancing effect of reducing the dc current to stay on the same step is no longer effective. Thus, such steps oscillate rapidly with the microwave power. For a given microwave current, the nth-order step is zero when increasing the dc current on the top of the $(n-1)$th step makes a positive 2π rotation to appear and a negative 2π rotation to disappear at the same time. This explains why in this range of the I-V curves, voltage jumps of two steps are often observed. The absence of the dc current counterbalancing effect makes the steps stay at the same dc current value while oscillating with microwave power. Furthermore, they are located along the ohmic line since this type of step occurs only in range III. In fact, these oscillating steps exhibit a Bessel-function-like behavior which is to be expected from Eq. (1) for large microwave bias currents.

In conclusion, our experimental and numerical results have led us to an intuitive interpretation of Josephson junctions in the low-frequency and damped regime. The adiabatic interpretation has been proven to be useful for understanding the main features of the I-V characteristics, i.e., the overall shape and the two different behaviors of the Shapiro steps. The low-frequency regime is very common experimentally because the characteristic frequency is usually quite high (for $R=1\ \Omega$ and $I_c=1$ mA, ω_c is already as large as 500 Ghz). In the high-frequency regime ($\omega>\omega_c$) the adiabatic approximation fails and it is well known that a Bessel-function behavior of the steps is to be expected from Eq. (1). Although this adiabatic description is presented for the case of simple RSJ model without capacitance, we have checked that a small capacitative term does not modify the picture as long as $\beta_c<1$. For $\beta_c>1$, the plasma oscillations become important so that more complicated behavior of the junction is to be expected. This is especially true for the chaotic regimes, and their influence on the I-V characteristics will have to be included. Such complications and their effects on the I-V curves are currently being investigated by using a physical model similar to the one reported here.

ACKNOWLEDGMENTS

We would like to acknowledge Dr. R. B. Laibowitz for critically reading this manuscript. One of us (C.V.) would also like to thank Dr. A. P. Malozemoff and Dr. R. B. Laibowitz for their hospitality during his visit at the IBM Thomas J. Watson Research Center.

---

*Permanent address: Laboratoire de Physique de la Matière Condensée (L.A. 190), Université de Nice, F-06034 Nice Cedex, France.

[1]S. Shapiro, Phys. Rev. Lett. **11**, 80 (1963).

[2]H. Fack and V. Kose, J. Appl. Phys. **42**, 320 (1971).

[3]P. Russer, J. Appl. Phys. **43**, 2008 (1972).

[4]K. H. Brown, A. C. Callegari, M. M. Chen, J. H. Greiner, H. C. Jones, M. B. Ketchen, K. K. Kim, A. W. Kleinsasser, H. A. Notarys, G. Proto, R. H. Wang, and T. Yogi (unpublished).

[5]D. E. McCumber, J. Appl. Phys. **39**, 3113 (1968).

[6]D. D'Humieres, M. R. Beasley, B. A. Huberman, and A. Libchaber, Phys. Rev. A **26**, 3483 (1982).

[7]R. Gross, H. Seifert, R. P. Huebener, and K. Yoshida, J. Low Temp. Phys. **54**, 277 (1984).